



α -D-Glcp-(1 \leftrightarrow 1)- β -D-Galp-containing oligosaccharides, novel products from lactose by the action of β -galactosidase

Carel T.M. Fransen^a, Katrien M.J. Van Laere^b, Arjan A.C. van Wijk^a,
Lars P. Brüll^c, Mark Dignum^b, Jane E. Thomas-Oates^c, Johan Haverkamp^c,
Henk A. Schols^b, Alphons G.J. Voragen^b, Johannes P. Kamerling^a,
Johannes F.G. Vliegthart^{a,*}

^a *Bijvoet Center, Department of Bio-Organic Chemistry, Utrecht University, PO Box 80075,
NL-3508 TB Utrecht, Netherlands*

^b *Food Science Group, Wageningen Agricultural University, PO Box 8129, NL-6700 EV Wageningen, Netherlands*

^c *Bijvoet Center, Department of Mass Spectrometry, Utrecht University, Sorbonnelaan 16,
NL-3584 CA Utrecht, Netherlands*

Received 5 August 1998; accepted 26 October 1998

Abstract

A mixture of oligosaccharides produced by β -galactosidase using lactose as a substrate was fractionated according to degree of polymerization using gel filtration, followed by high-pH anion-exchange chromatography. The fractions obtained were analyzed using monosaccharide analysis, methylation analysis, mass spectrometry, and NMR spectroscopy. Twelve novel non-reducing oligosaccharides were characterized, namely, $[\beta$ -D-Galp-(1 \rightarrow 4)]_n- α -D-Glcp-(1 \leftrightarrow 1)- β -D-Galp[-(4 \leftarrow 1)- β -D-Galp]_m, with $n, m = (1, 2, 3, \text{ or } 4)$ and β -D-Galp-(1 \rightarrow 2)- α -D-Glcp-(1 \leftrightarrow 1)- β -D-Galp. © 1998 Elsevier Science Ltd. All rights reserved.

Keywords: β -Galactosidase; Transgalactosylation; Functional food; Non-reducing galacto-oligosaccharides; Oligogalactosylated glucoses; Primary structure analysis

1. Introduction

Galacto-oligosaccharides, including the oligogalactosylated glucoses, are claimed to be beneficial for human health because they seem to promote the growth of bifidobacteria in the large intestine [1]. Several studies suggest that the volatile fatty acids resulting from the fermentation of galacto-oligosaccharides by the

intestinal microflora improve the absorption ability of the intestinal epithelium [2–4].

Oligogalactosylated glucoses can be prepared from lactose through the transgalactosylating activity of β -galactosidase (EC 3.2.1.23). Various parameters such as source of the enzyme, substrate concentration, pH, and temperature can influence the transgalactosylation and thereby the final yields of the different compounds formed [5]. The structures of oligogalactosylated glucoses reported so far range from dimers to pentamers [1,6–9]. Depending on the biological origin of the β -galactosidase applied, different linkages be-

* Corresponding author. Tel.: +31-30-2532168/2184; fax: +31-30-2540980.

E-mail address: vlieg@cc.uu.nl (J.F.G. Vliegthart)

tween Gal and the reducing Glc unit have been identified, namely, β -D-Galp-(1 \rightarrow 2)-D-Glcp, β -D-Galp-(1 \rightarrow 3)-D-Glcp, β -D-Galp-(1 \rightarrow 4)-D-Glcp, and β -D-Galp-(1 \rightarrow 6)-D-Glcp. Branched Glc residues also occur, whereas the oligogalactose fragments contain mainly (1 \rightarrow 4) or (1 \rightarrow 6) linkages. So far oligogalactosylated glucose tetramers and pentamers have rarely been observed in large amounts.

Here, we report on a novel transgalactosylating activity of β -galactosidase leading to the formation of α -D-Glcp-(1 \leftrightarrow 1)- β -D-Galp elements in several oligogalactosylated glucoses.

2. Results

Purification of oligosaccharides produced by β -galactosidase.—The oligogalactosylated glucose sample supplied (Borculo Whey Products) was fractionated by gel-permeation chromatography using Fractogel TSK HW-40(S) followed by Bio-Gel P-2. Following this protocol, fractions of different degrees of polymerization were obtained. These pools of oligosaccharides were further fractionated by high-performance anion-exchange chromatography (HPAEC). In Fig. 1 HPAEC profiles of the starting oligogalactosylated glucose sample (upper panel) and of five Bio-Gel P-2 fractions (dimers to hexamers) are shown. The major components [$(\beta$ -D-Galp-(1 \rightarrow 4))_n-D-Glcp, and $(\beta$ -D-Galp-(1 \rightarrow 6))_n- β -D-Galp-(1 \rightarrow 4)-D-Glcp, $n=0-5$] in each Bio-Gel P-2 fraction were characterized using HPAEC retention times and ^1H NMR spectroscopy (data not shown). The oligogalactosylated glucose structures found were in agreement with those reported so far [5]. For the NMR analysis, use was made of the chemical shifts of linear β -(1 \rightarrow 4)-linked D-galactobi- to pentaose (see Table 1). The ^1H and ^{13}C chemical shifts of the latter compounds, which have not been reported so far in detail, are shown in Tables 1 and 2, respectively. Additionally to the known oligogalactosylated glucoses, each Bio-Gel P-2 fraction contained at least one less retarded component (Fig. 1, indicated by its fraction number) whose structure has not yet been reported. The structural characterization of these compounds is described in the following paragraphs.

Characterization of Fractions 2.1 and 2.2.—The pool of disaccharides contained, according to the HPAEC chromatogram, at least six components (Fig. 1). The ^1H NMR spectrum of Fraction 2.2 indicated the presence of free Gal and Glc (data not shown). Fraction 2.1 contained a disaccharide consisting of Glc and Gal in a molar ratio of 1:1. Methylation analysis revealed the presence of equimolar amounts of terminal Galp and terminal Glcp. Electrospray ionization mass spectrometry (ESMS) analysis of the sodium borodeuteride-treated and permethylated Fraction 2.1 showed an ion at m/z 477 (data not shown), corresponding to a sodium-cationized pseudo-molecular ion $[\text{M} + \text{Na}]^+$ for nonreduced permethylated Hex₂. The $[\text{M} + \text{H}]^+$ ion at m/z 455, observed in the FAB mass spectrum was used for a high energy collision experiment applying fast atom bombardment collision induced dissociation tandem mass spectrometry (FAB CID MS-MS). The most abundant and the only mass spectrometric sequence ion notable in the tandem mass spectrum was the B₁

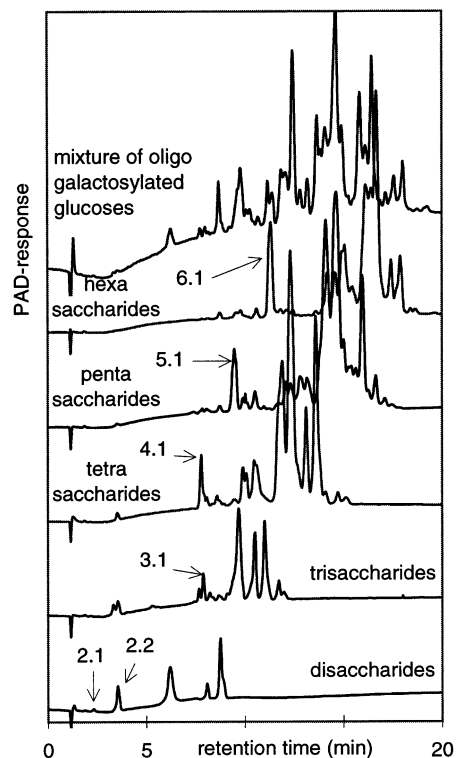


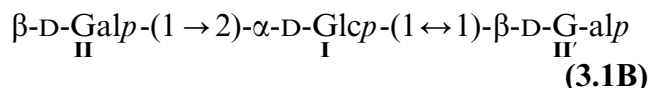
Fig. 1. HPAEC profiles of the starting galactosylated glucose sample (upper panel, as obtained from Borculo Whey Products) and of the different Bio-Gel P-2 fractions (disaccharides through hexasaccharides).

Quantitative monosaccharide analysis of Fraction 3.1 revealed Glc and Gal in a molar ratio of 1.0:1.9. Methylation analysis demonstrated the presence of terminal Galp and 4-substituted Glcp residues. In the ESMS spectrum of the sodium borodeuteride-treated and permethylated Fraction 3.1, an ion at m/z 681 was observed, corresponding to $[M + Na]^+$ for a nonreduced permethylated Hex₃. The most abundant ions observed in the tandem mass spectrum obtained from the protonated derivatized oligosaccharide, m/z 659, were the B₁ and B₂ ions (m/z 219 and 423). The intense ion observed at m/z 455 corresponding in mass to fully methylated Hex₂ was assigned as resulting from 'internal residue loss' [11]. The very low abundance of the ion at m/z 627 corresponding to the loss of methanol from the precursor and having the same mass as a B₃ ion was consistent with the presence of a (1↔1) glycosidic linkage in Hex₃.

1D ¹H NMR analysis of Fraction 3.1 (Fig. 2(B)) showed three, equally intense, anomeric signals at δ 5.228 (³J_{1,2} 3.4 Hz, ¹J_{C-1,H-1} 173 Hz), 4.576 (³J_{1,2} 7.0 Hz, ¹J_{C-1,H-1} 160 Hz), and 4.443 (³J_{1,2} 7.9 Hz, ¹J_{C-1,H-1} 163 Hz). Taking into account both the ³J_{1,2} and ¹J_{C-1,H-1} (from HMBC) coupling constants, the first signal belonged to an α and the other two to β gluco/galactopyranosyl residues. 2D NMR spectroscopy (DQF COSY, TOCSY, and ROESY) together with the chemical shift values of 1–4 allowed the assignment of all proton resonances, as presented in Table 3. In this way, the α anomeric signal could be assigned to the Glcp residue and the β anomeric signals to Galp residues. The linkages between the different monosaccharide units were con-

firmed by the interresidual ROESY cross-peaks II H-1, I H-4 and I H-1, II' H-1, and by the long range HMBC contacts (Fig. 3) II H-1, I C-4, I H-4, II C-1, I H-1, II' C-1, and II' H-1, I C-1. The assignments of the carbon chemical shifts as obtained from the HMBC spectrum are shown in Table 4. They are in agreement with terminal β -Galp (C-1, δ 103.8 and 104.4) and 4-substituted α -Glcp (C-1, δ 101.7; C-4, δ 79.0).

In the 1D ¹H NMR spectrum of Fraction 3.1 (Fig. 2(B)) some other anomeric signals with much lower intensity (ca. 10%) were visible (δ 5.45, ³J_{1,2} 3.4 Hz; 4.62, 7.2 Hz; 4.53, 7.0 Hz), suggesting the presence of compound **3.1B**:



A series of ¹H chemical shift values of low intensity peaks (Table 3) could be assigned from the different 2D spectra recorded of Fraction 3.1. Evidence for structure **3.1B** was found in the ROESY spectrum, showing a strong ROE I H-1, II' H-1 and a weak ROE II H-1, I H-2. The substitution of Glc at O-2 is supported by the chemical shift of the anomeric proton of residue I (α H-1, 5.45 ppm) which is characteristic for a 2-substituted α -Glc residue [8]. No 2-substituted hexose was found in the methylation analysis, probably because of the small amount of this compound present in Fraction 3.1.

Characterization of Fraction 4.1.— Monosaccharide analysis of Fraction 4.1 revealed the presence of Glc and Gal in a molar ratio of 1.3:2.7. In the ESMS spectrum of the sodium borodeuteride-treated and permethyl-

Table 2

¹³C chemical shifts of β -D-Galp-(1→4)- β -D-Galp-(1→4)- β -D-Galp-(1→4)-D-Galp (**3**)^a

Compound	Residue	C-1	C-2	C-3	C-4	C-5	C-6
3	β -D-Galp-(1→4)- β -D-Galp-(1→4)- β -D-Galp-(1→4)-D-Galp	105.18	72.26	73.64	69.51	76.04	61.87 ^d
	4)- β -D-Galp-(1→4)- β -D-Galp-(1→4)- β -D-Galp-(1→4)-D-Galp	105.23	72.69 ^b	74.13	78.01	75.39 ^c	61.61 ^d
	4)- β -D-Galp-(1→4)- β -D-Galp-(1→4)- β -D-Galp-(1→4)-D-Galp	105.23	72.73 ^b	74.17	78.45	75.34 ^c	61.61 ^d
	4)- α -D-Galp	93.20	70.74	70.59	79.72	69.71	61.77 ^d
	4)- β -D-Galp	97.29	72.78	73.13	78.75	75.20	69.44 ^d

^a Assignments were obtained from a 1D ¹³C and a HMBC experiment recorded at 75 and 500 MHz, respectively.^b Assignments may have to be interchanged.^c See footnote b.^d See footnote b.

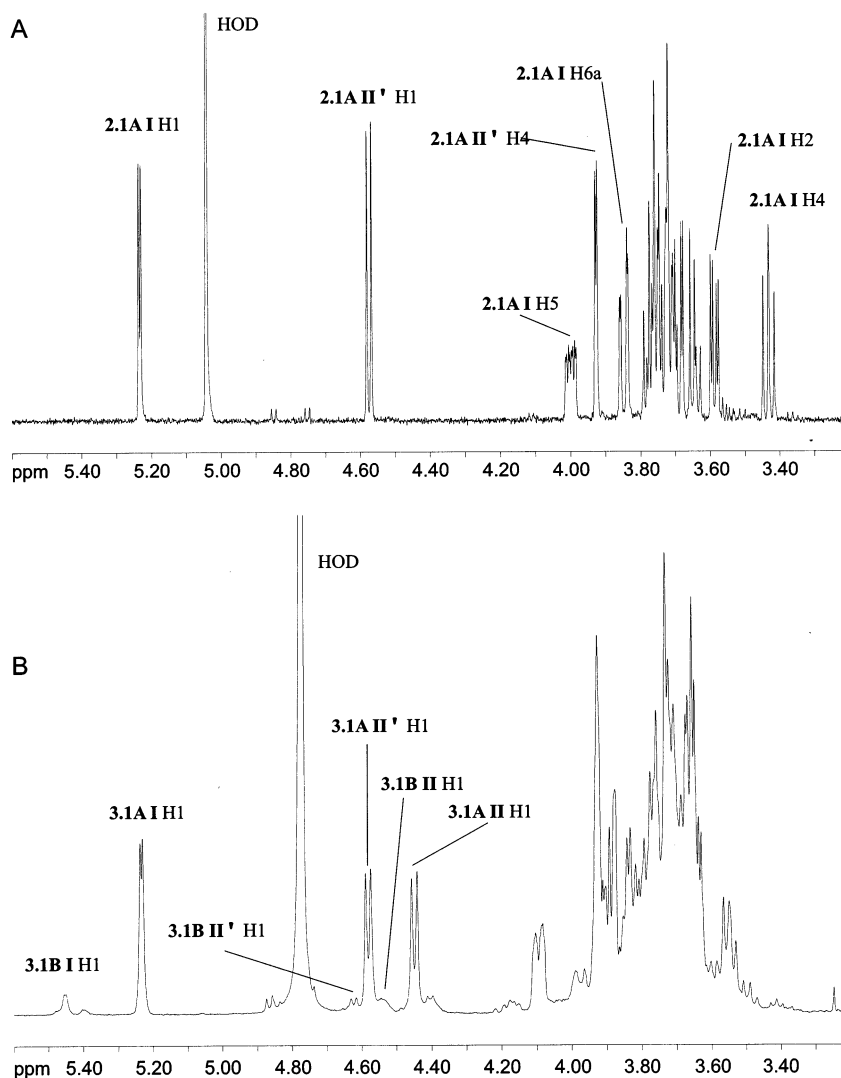


Fig. 2. 1D ^1H NMR spectrum of (A) Fraction 2.1 (600 MHz, 278 K) and (B) Fraction 3.1 (500 MHz, 300 K). Assignments are as follows: **3.1A I H1** means H-1 of residue I of compound **3.1A**.

ated Fraction 4.1, an ion at m/z 885 was observed, corresponding to $[\text{M} + \text{Na}]^+$ for a nonreduced permethylated Hex_4 .

In the 1D ^1H NMR spectrum of Fraction 4.1 (Fig. 4(A)) two almost equally intense H-1 α signals around 5.22 ppm are present. The TOCSY spectrum showed that both signals belong to Glcp residues. Because these oligosaccharides were synthesized by β -galactosidase action, each oligosaccharide can only contain one Glc unit, and, consequently, this fraction contains at least two components. The H-1 β signals were assigned to Galp residues based on their TOCSY spin system. The ROESY spectrum showed for each H-1 α signal an interresidual contact to a H-1 β signal. One of these β -Galp residues (δ 4.571)

was not substituted whereas the other (δ 4.60) was substituted at O-4 (H-4 at δ 4.18 instead of \sim 3.90; see Table 1). In total, two 4-substituted Galp residues were found (H-1, δ 4.478 with H-4, δ 4.18; H-1, δ 4.60 with H-4, δ 4.18). The typical chemical shifts of two H-1 β signals below δ 4.50 (δ 4.478 and 4.439) indicated the presence of two Galp residues linked to O-4 of a Glcp residue [8,12] (structure **3.1A**).

On the basis of the results above, the following two structures, **4.1A** and **4.1B**, can be established:

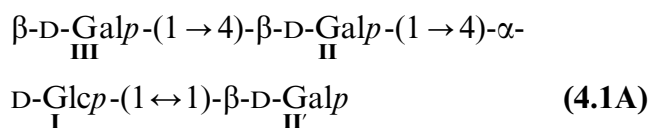


Table 3

¹H NMR chemical shifts of analyzed oligogalactosylated glucoses (recorded at 300 K, at 500 or 600 MHz)

Compound	Residue	H-1	H-2	H-3	H-4	H-5	H-6a, 6b	
2.1A	I	α-D-Glcp-(1↔	5.230	3.585	3.76	3.429	3.992	3.84, 3.74
	II'	1)-β-D-Galp	4.571	3.63	3.68	3.924	3.72	
3.1A	II	β-D-Galp-(1→	4.443	3.55	3.65	3.92	3.70	3.73–3.78
	I	4)-α-D-Glcp-(1↔	5.228	3.64	3.88	3.69	4.09	3.82–3.88
3.1B	II'	1)-β-D-Galp	4.576	3.64	3.67	3.92	3.71	3.71–3.76
	II	β-D-Galp-(1→	4.53	3.63	3.63	3.92		
4.1A	I	2)-α-D-Glcp-(1↔	5.45	3.72	3.92	3.65	4.16	
	II'	1)-β-D-Galp	4.62	3.64	3.67	3.91		
	III	β-D-Galp-(1→	4.59	3.57 ^b	3.65	3.89	3.67	3.67–3.80
4.1B	II	4)-β-D-Galp-(1→	4.478	3.61	3.77	4.18	3.68	3.67–3.80
	I	4)-α-D-Glcp-(1↔	5.216	3.64	3.85	3.70	4.04	3.83–3.89
	II'	1)-β-D-Galp	4.571	3.64	3.67	3.92	3.71	3.67–3.80
	II	β-D-Galp-(1→	4.439	3.53	3.66	3.91	3.65	3.67–3.80
5.1A	I	4)-α-D-Glcp-(1↔	5.223	3.63	3.88	3.69	4.08	3.82–3.88
	II'	1)-β-D-Galp-(4	4.60	3.71	3.78	4.18	3.68	3.83–3.89
	III'	← 1)-β-D-Galp	4.59	3.60 ^b	3.65	3.89	3.67	3.67–3.80
	IV	β-D-Galp-(1→	4.60	3.58	3.66	3.89	3.68	3.72–3.87
	III	4)-β-D-Galp-(1→	4.646	3.65	3.77	4.19	3.72	3.72–3.87
5.1B	II	4)-β-D-Galp-(1→	4.484	3.62	3.78	4.20	3.69	3.72–3.87
	I	4)-α-D-Glcp-(1↔	5.216	3.64	3.89	3.71	4.04	3.81–3.87
	II'	1)-β-D-Galp	4.58	3.63	3.68	3.90	3.72	3.72–3.87
	III	β-D-Galp-(1→	4.60	3.58	3.66	3.89	3.76	3.72–3.87
	II	4)-β-D-Galp-(1→	4.484	3.62	3.78	4.20	3.69	3.72–3.87
5.1C	I	4)-α-D-Glcp-(1↔	5.221 ^a	3.64	3.89	3.71	4.10	3.81–3.87
	II'	1)-β-D-Galp-(4	4.61	3.71	3.79	4.21	3.76	3.72–3.87
	III'	← 1)-β-D-Galp	4.60	3.58	3.66	3.90	3.76	3.72–3.87
	II	β-D-Galp-(1→	4.445	3.56	3.65	3.92	3.71	3.72–3.87
	I	4)-α-D-Glcp-(1↔	5.227 ^a	3.64	3.89	3.70	4.10	3.81–3.87
6.1A	II'	1)-β-D-Galp-(4	4.61	3.71	3.79	4.21	3.76	3.72–3.87
	III'	← 1)-β-D-Galp-(4	4.651	3.65	3.77	4.19	3.72	3.72–3.87
	IV'	← 1)-β-D-Galp	4.60	3.58	3.66	3.90	3.76	3.72–3.87
	V	β-D-Galp-(1→	4.605	3.59	3.67	3.91	3.77	3.69–3.86
	IV	4)-β-D-Galp-(1→	4.65–4.67	3.66–3.69	3.74	4.18–4.19	3.72–3.73	3.69–3.86
6.1B	III	4)-β-D-Galp-(1→	4.65–4.67	3.66–3.69	3.74	4.18–4.19	3.72–3.73	3.69–3.86
	II	4)-β-D-Galp-(1→	4.487	3.64	3.79	4.20	3.70	3.69–3.86
	I	4)-α-D-Glcp-(1↔	4.487	3.64	3.79	4.20	3.70	3.69–3.86
	II'	1)-β-D-Galp	4.582	3.64	3.68	3.94	4.11	3.81–3.90
	IV	β-D-Galp-(1→	4.605	3.59	3.67	3.91	3.77	3.69–3.86
6.1C	III	4)-β-D-Galp-(1→	4.65–4.67	3.66–3.69	3.74	4.18–4.19	3.72–3.73	3.69–3.86
	II	4)-β-D-Galp-(1→	4.487	3.64	3.79	4.20	3.70	3.69–3.86
	I	4)-α-D-Glcp-(1↔	5.229 ^c	3.64	3.88	3.71	4.06	3.81–3.90
	II'	1)-β-D-Galp-(4	4.610	3.72–3.74	3.81	4.21	3.77–3.78	3.69–3.86
	III'	← 1)-β-D-Galp	4.605	3.59	3.67	3.91	3.77	3.69–3.86
6.1D	III	β-D-Galp-(1→	4.605	3.59	3.67	3.91	3.77	3.69–3.86
	II	4)-β-D-Galp-(1→	4.487	3.64	3.79	4.20	3.70	3.69–3.86
	I	4)-α-D-Glcp-(1↔	5.232 ^c	3.64	3.88	3.71	4.06	3.81–3.90
	II'	1)-β-D-Galp-(4	4.610	3.72–3.74	3.81	4.21	3.77–3.78	3.69–3.86
	III'	← 1)-β-D-Galp-(4	4.65–4.67	3.66–3.69	3.74	4.18–4.19	3.72–3.73	3.69–3.86
6.1D	IV'	← 1)-β-D-Galp	4.605	3.59	3.67	3.91	3.77	3.69–3.86
	II	β-D-Galp-(1→	4.429	3.56	3.67	3.93		3.69–3.86
	I	4)-α-D-Glcp-(1↔	5.23	3.64	3.88	3.71	4.06	3.81–3.90
	II'	1)-β-D-Galp-(4	4.610	3.72–3.74	3.81	4.21	3.77–3.78	3.69–3.86
	III'	← 1)-β-D-Galp-(4	4.65–4.67	3.66–3.69	3.74	4.18–4.19	3.72–3.73	3.69–3.86
6.1D	IV'	← 1)-β-D-Galp-(4	4.65–4.67	3.66–3.69	3.74	4.18–4.19	3.72–3.73	3.69–3.86
	V'	← 1)-β-D-Galp	4.605	3.59	3.67	3.91	3.77	3.69–3.86

^a Assignments may have to be interchanged.^b See footnote a.^c See footnote a.

Table 4

¹³C NMR chemical shifts of analyzed oligogalactosylated glucoses (recorded at 300 K, at 125 or 150 MHz)

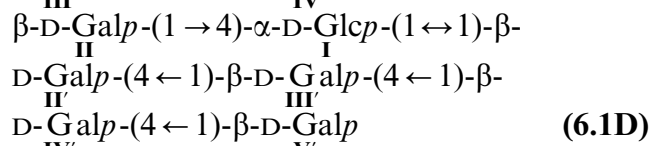
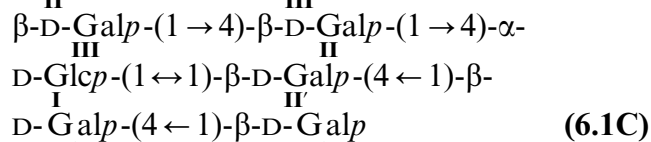
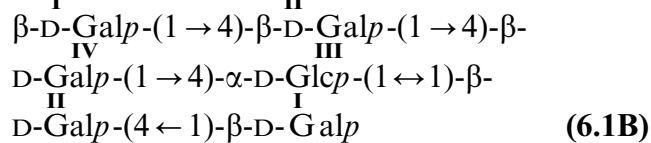
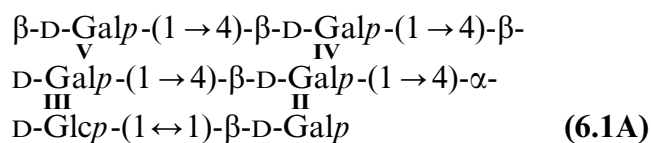
Compound	Residue	C-1	C-2	C-3	C-4	C-5	C-6	
2.1A	I	α -D-Glcp-(1 \leftrightarrow	101.1	72.1	73.4	70.2	73.2	61.1
	II'	1)- β -D-Galp	104.5	71.4	72.9	69.1	76.1	61.7
3.1A	II	β -D-Galp-(1 \rightarrow	103.8	71.9	73.4	69.4	76.4	61.8
	I	4)- α -D-Glcp-(1 \leftrightarrow	101.7	72.1	72.6	79.0	72.2	60.8
4.1A	II'	1)- β -D-Galp	104.4	71.6	73.2	69.2	76.4	61.8
	III	β -D-Galp-(1 \rightarrow	105.4	72.7	73.9	70.0	76.4	62–63
4.1B	II	4)- β -D-Galp-(1 \rightarrow	104.0	72.6	74.1	78.3	76.4	62–63
	I	4)- α -D-Glcp-(1 \leftrightarrow	101.5	72.4	72.7	79.1	72.7	61.0
5.1A	II'	1)- β -D-Galp	104.7	72.9	73.6	69.8	76.7	62–63
	II	β -D-Galp-(1 \rightarrow	104.0	72.1	73.8	69.9	76.3	62–63
5.1B	I	4)- α -D-Glcp-(1 \leftrightarrow	101.1	72.4	72.7	79.3	72.6	61.0
	II'	1)- β -D-Galp-(4	104.8	72.4	74.0	78.3	76.4	62–63
5.1C	III'	\leftarrow 1)- β -D-Galp	105.4	72.7	73.9	70.0	76.4	62–63
	IV	β -D-Galp-(1 \rightarrow	105.0	72.2	73.5	69.5	75.4	61.5–61.9
5.1B	III	4)- β -D-Galp-(1 \rightarrow	105.0	72.0	73.9	78.0	76.2	61.5–61.9
	II	4)- β -D-Galp-(1 \rightarrow	103.6	72.1	73.7	78.3	76.1	61.5–61.9
5.1C	I	4)- α -D-Glcp-(1 \leftrightarrow	100.8	72.6	72.2	79.1	72.2	60.9
	II'	1)- β -D-Galp	104.2	72.2	73.4	69.4	75.2	61.5–61.9
5.1B	III	β -D-Galp-(1 \rightarrow	105.0	72.2	73.5	69.5	75.4	61.5–61.9
	II	4)- β -D-Galp-(1 \rightarrow	103.6	72.1	73.7	78.3	76.1	61.5–61.9
5.1C	I	4)- α -D-Glcp-(1 \leftrightarrow	100.6	72.6	72.2	79.1	72.1	60.9
	II'	1)- β -D-Galp-(4	104.2	71.9	73.6	77.8	76.0	61.5–61.9
5.1C	III'	\leftarrow 1)- β -D-Galp	105.0	72.2	73.5	69.5	75.4	61.5–61.9
	II	β -D-Galp-(1 \rightarrow	103.6	72.2	73.5	69.2	75.2	61.5–61.9
5.1C	I	4)- α -D-Glcp-(1 \leftrightarrow	100.6	72.6	72.2	79.1	72.1	60.9
	II'	1)- β -D-Galp-(4	104.2	71.9	73.6	77.8	76.0	61.5–61.9
5.1C	III'	\leftarrow 1)- β -D-Galp-(4	105.0	72.0	73.9	78.0	76.2	61.5–61.9
	IV'	\leftarrow 1)- β -D-Galp	105.0	72.2	73.5	69.5	75.4	61.5–61.9
6.1A	V	β -D-Galp-(1 \rightarrow	105.2	71.5–74	71.5–74	69.6	75.6	61.5–62
	IV	4)- β -D-Galp-(1 \rightarrow	105.2	71.5–74	71.5–74	78.1–78.5	75.4	61.5–62
6.1B	III	4)- β -D-Galp-(1 \rightarrow	105.2	71.5–74	71.5–74	78.1–78.5	75.4	61.5–62
	II	4)- β -D-Galp-(1 \rightarrow	103.8	71.5–74	71.5–74	78.1–78.5	76.2	61.5–62
6.1B	I	4)- α -D-Glcp-(1 \leftrightarrow	100.8	72.8	72.4	79.2	72.5	60.8
	II'	1)- β -D-Galp	104.5	71.5–74	71.5–74	69.4	75.6	61.5–62
6.1B	IV	β -D-Galp-(1 \rightarrow	105.2	71.5–74	71.5–74	69.6	75.6	61.5–62
	III	4)- β -D-Galp-(1 \rightarrow	105.2	71.5–74	71.5–74	78.1–78.5	75.4	61.5–62
6.1B	II	4)- β -D-Galp-(1 \rightarrow	103.8	71.5–74	71.5–74	78.1–78.5	76.2	61.5–62
	I	4)- α -D-Glcp-(1 \leftrightarrow	101.0	72.8	72.4	79.2	72.5	60.8
6.1B	II'	1)- β -D-Galp-(4	104.5	71.5–74	71.5–74	77.9	75.6	61.5–62
	III'	\leftarrow 1)- β -D-Galp	105.2	71.5–74	71.5–74	69.6	75.6	61.5–62
6.1C	III	β -D-Galp-(1 \rightarrow	105.2	71.5–74	71.5–74	69.6	75.6	61.5–62
	II	4)- β -D-Galp-(1 \rightarrow	103.8	71.5–74	71.5–74	78.1–78.5	76.2	61.5–62
6.1C	I	4)- α -D-Glcp-(1 \leftrightarrow	101.0	72.8	72.4	79.2	72.5	60.8
	II'	1)- β -D-Galp-(4	104.5	71.5–74	71.5–74	77.9	75.6	61.5–62
6.1C	III'	\leftarrow 1)- β -D-Galp-(4	105.2	71.5–74	71.5–74	78.1–78.5	75.4	61.5–62
	IV'	\leftarrow 1)- β -D-Galp	105.2	71.5–74	71.5–74	69.6	75.6	61.5–62
6.1D	II	β -D-Galp-(1 \rightarrow	104.3	71.5–74	71.5–74	69.4	75.6	61.5–62
	I	4)- α -D-Glcp-(1 \leftrightarrow	101.0	72.8	72.4	79.2	72.5	60.8
6.1D	II'	1)- β -D-Galp-(4	104.5	71.5–74	71.5–74	77.9	75.6	61.5–62
	III'	\leftarrow 1)- β -D-Galp-(4	105.2	71.5–74	71.5–74	78.1–78.5	75.4	61.5–62
6.1D	IV'	\leftarrow 1)- β -D-Galp-(4	105.2	71.5–74	71.5–74	78.1–78.5	75.4	61.5–62
	V'	\leftarrow 1)- β -D-Galp	105.2	71.5–74	71.5–74	69.6	75.6	61.5–62

tion 5.1 with those obtained for Fractions 3.1 and 4.1, the signal at δ 4.445 was assigned to terminal β -Galp (compound **5.1C**) and that at δ 4.484 to 4-substituted β -Galp linked to O-4 of α -Glc (compounds **5.1A** and **5.1B**). According to the ROESY and TOCSY data only terminal and 4-substituted β -Galp residues occur in this fraction (terminal β -Galp H-4, $\delta \sim 3.90$; 4-substituted β -Galp H-4, $\delta \sim 4.20$), and each α -Glc H-1 signal (δ 5.216, 5.221, 5.227; Table 3) has an interresidual ROESY cross-peak to a β -Galp H-1 resonance. The chemical shift of C-1 (δ 100.6–100.8; Table 4) gives supporting evidence for the substitution of the anomeric centers of the α -Glc residues.

Based on the reasoning presented above, the structure with the β -Gal H-1 signal at δ 4.445 is **5.1C**. The α -Glc H-1 doublet at δ 5.216 has a ROESY cross-peak with a β -Galp H-1 signal at δ 4.58. According to the TOCSY

spectrum this Galp residue occurs in a terminal position (H-4, δ 3.90), thereby indicating structure **5.1A**. The third component has structural similarities with **5.1A** and **5.1C** (i.e., the presence of the following structural elements: β -Galp-(1 \rightarrow 4)- β -Galp and β -Galp-(1 \rightarrow 4)- α -Glc-(1 \leftrightarrow 1)- β -Galp) giving rise to overlap in the NMR spectra (compare Table 1). These similarities lead to propose the presence of structure **5.1B**.

Characterization of Fraction 6.1.—Structural analysis of Fraction 6.1 gave evidence for the occurrence of compounds **6.1A**, **6.1B**, **6.1C**, and **6.1D**.



Monosaccharide analysis revealed the presence of Gal and Glc in a molar ratio of 4.9:1.1. Methylation analysis showed the occurrence of terminal Gal, 4-substituted Gal, and 4-substituted Glc. In the ESMS spectrum of the sodium borodeuteride-treated and permethylated Fraction 6.1, an ion at m/z 1293 was observed, corresponding to $[M + Na]^+$ for a nonreduced permethylated Hex₆.

TOCSY, ROESY, and seHSQC experiments revealed the presence of the structural elements β -Galp-(1 \rightarrow , \rightarrow 4)- β -Galp-(1 \rightarrow , and \rightarrow 4)- α -Glc-(1 \rightarrow). In the 1D ¹H NMR spectrum of Fraction 6.1 (Fig. 5) the doublet at δ 4.429 is characteristic for a terminal β -Galp residue (1 \rightarrow 4)-linked to α -Glc (see compounds **5.1C** and **4.1B**) and the doublet with the same intensity at δ 3.93 is typical for H-4 of a terminal β -Galp residue, giving rise to structure **6.1D**. The H-1 α region ($\delta \sim 5.23$) is

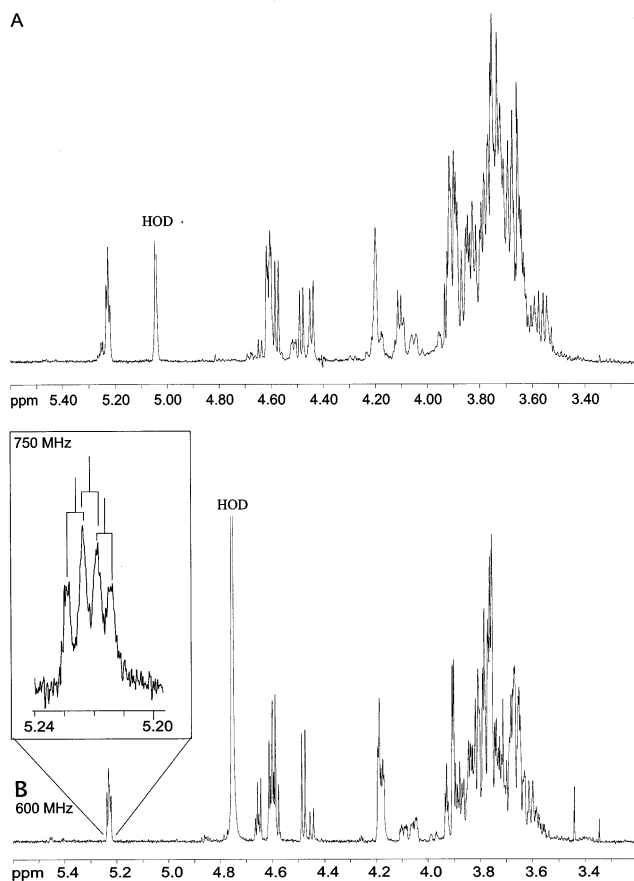


Fig. 4. 1D ¹H NMR spectrum of (A) Fraction 4.1 (600 MHz, 278 K) and (B) Fraction 5.1 (600 MHz, 300 K). The enlargement in the spectrum of Fraction 5.1 contains the corresponding region in the 750 MHz 1D ¹H spectrum of this fraction. The three α anomeric signals of compounds **5.1A**, **5.1B**, and **5.1C** are indicated.

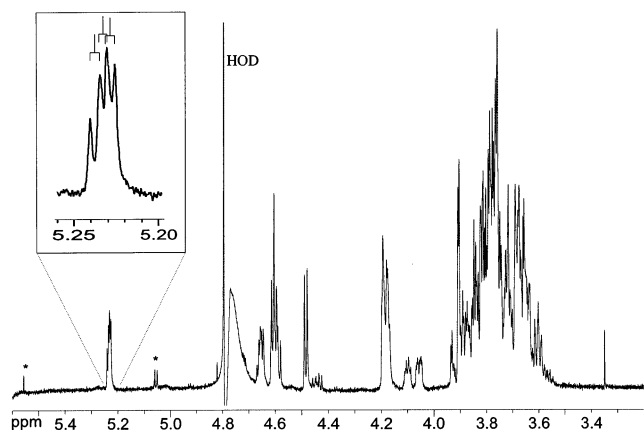


Fig. 5. 1D ^1H NMR spectrum of Fraction 6.1 (750 MHz, 298 K). The α anomeric signals are enlarged. * Peaks belong to non-carbohydrate impurities resonating between 1 and 3 ppm. They are folded to these positions due to the small spectral width used for the acquisition of this spectrum.

composed of three doublets with relative intensities 1:2:2, as indicated in Fig. 5. According to TOCSY and seHSQC data these doublets belong to α -Glc p H-1 atoms. Since each compound can only contain one Glc residue, Fraction 6.1 contains at least three compounds (see above). The doublet of **6.1D II** H-1 is hidden in the multiplet around $\delta \sim 5.23$. Therefore, the presence of four instead of three compounds is suggested. The H-1 β signal at $\delta 4.582$ is characteristic for terminal β -Gal p, (1 \leftrightarrow 1)-linked to α -Glc p (H-1, $\delta 5.238$) leading to structure **6.1A**. Compounds **6.1B** and **6.1C** have structural similarities with parts of **6.1A** (and the minor component **6.1D**) and with each other (i.e., the occurrence of the following structural elements: (β -Gal p (1 \rightarrow 4)) $_n$ - β -Gal p $n=0-2$ and β -Gal p (1 \rightarrow 4)- α -Glc p (1 \leftrightarrow 1)- β -Gal p) giving rise to overlap in the NMR spectra. By consequence, no complete assignment could be established. Exclusive evidence for their presence is the number of Glc H-1 α signals.

3. Discussion

This structural study of oligosaccharides produced by the transgalactosylation activity of β -galactosidase using lactose as a substrate, revealed the formation of a series of non-reducing oligosaccharides containing one α -Glc p unit and a variable number of β -Gal p units

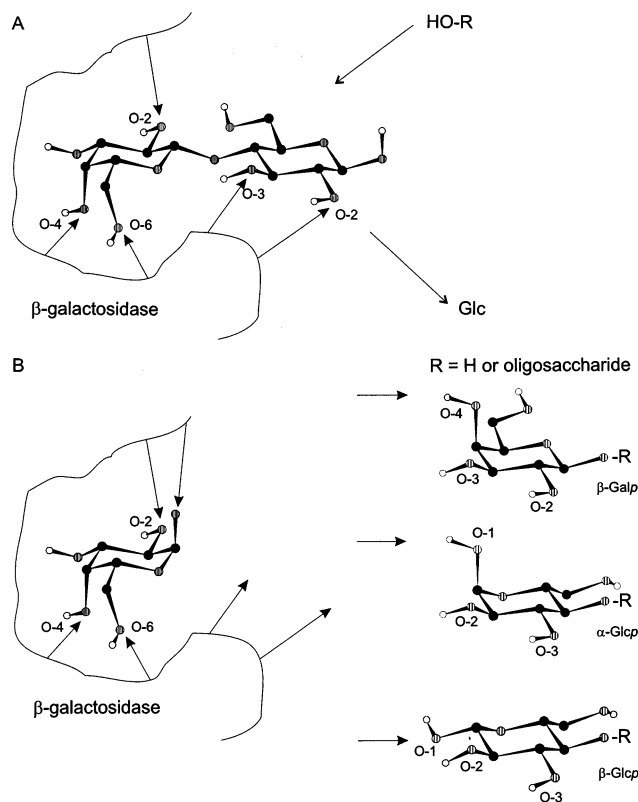


Fig. 6. (A) Proposed hydrogen bonding between β -galactosidase and lactose [13]. During the transgalactosylation process (B), the terminal residue of the galactosyl acceptor will be located in the same part of the pocket as Glc in a galactosidase reaction. Presumably, the orientation of the hydroxyl groups of the acceptor determine the ability of the enzyme to link Gal to a certain position.

having the structural motif α -D-Glc p-(1 \leftrightarrow 1)- β -D-Gal p in common. It would be interesting to investigate the gastrointestinal effect of galactosylated glucoses with respect to the Glc unit being reducing or not.

Interestingly, no β -Glc p was found in the nonreducing oligosaccharides described above. This can be explained by the way the enzyme binds to lactose [13]. According to [13] lactose can be positioned on the enzyme via several hydrophobic contacts and intermolecular hydrogen bonds (Fig. 6(A)) to Gal (O-2, O-4, and O-6) and Glc (O-2 and O-3). During the transgalactosylation process, the terminal Gal residue of the galactosyl acceptor is located in the same part of the pocket as Glc in a galactosidase reaction (Fig. 6(B)). Presumably the same intermolecular hydrogen bonds are present, as Gal is the C-4 epimer of Glc having a similar orientation of O-2 and O-3. This might explain the preference of the

enzyme for Gal O-4 in transgalactosylation reactions. When the anomeric center of Glc enters the active site as galactosyl acceptor, the orientation of Glc O-1,2,3 (Fig. 6(B)) depends on the anomeric configuration: for α -Glc the orientation is the same as for Gal O-4,3,2. This is probably the reason for the absence of β -Glc-containing nonreducing oligosaccharides.

4. Experimental

Model compounds.—Galactobiose to pentaose (1–4) were generated by a controlled digestion of soy arabinogalactan using endogalactanase from *A. niger* [14], then isolated via gel-permeation chromatography on Bio-Gel P-2, when necessary combined with HPAEC on CarboPac PA-100 [15].

Trans-galacto-oligosaccharides.—A mixture of galactosylated glucoses, produced by a pure β -galactosidase using lactose as substrate, was a gift of Borculo Whey Products (Borculo, The Netherlands). The sample supplied stemmed from an incubation mixture from which most of the free Gal and Glc and some di- and trisaccharide material had been removed by charcoal column chromatography. Inspection of the sample using gel-permeation chromatography on Bio-Gel P-2 showed that the material consisted of di- through hexasaccharides in a relative abundance of 3, 6, 17, 37, and 26%, respectively, whereas 11% of the material consisted of larger oligomers. The non-reducing oligosaccharide-containing fractions comprised 0.3, 0.3, 0.5, 4.6, 2.6% of di-through hexasaccharides, respectively, in the total mixture of oligosaccharides.

Purification of the galactosylated glucoses sample.—The galactosylated glucoses sample was fractionated on two connected columns (each 600 \times 26 mm) packed with Fractogel TSK HW-40(S) (25–40 μ m, E. Merck, Darmstadt, Germany), thermostated at 60 °C and eluted with water (2 mL/min), using a Pharmacia Hiload system equipped with a Pharmacia P50 pump. A Shodex RI-72 detector was used to monitor the refractive index. The various fractions were subfractionated on a Bio-Gel P-2 column (100 \times 2.8 cm) at 60 °C,

eluted with water; the elution profile was established via an auto-analyser (Skalar Analytical BV, Breda, The Netherlands) using the orcinol–H₂SO₄ assay for neutral sugars [16]. Further fractionation of Bio-Gel P-2 fractions was performed by HPAEC on a preparative (Fractions 2, 3, and 6) or a semi-analytical (Fractions 4 and 5) scale.

Preparative HPAEC was performed using a Spectra Physics P4000 pump equipped with a CarboPac PA-100 column (250 \times 22 mm) and coupled with a Spectra Physics AS3000 autosampler (900 μ L samples; flow rate, 20 mL/min) and a pulsed electrochemical detector (PED). Gradients were optimized for each sample using 0.2 M NaOH, 2 M NaOAc in 0.2 M NaOH and Millipore water as eluents. The effluent actually passing the detector was reduced to 1 mL/min by splitting the effluent post-column, and 10 mL fractions were collected and immediately neutralized by on-line addition of 1 M HOAc. Relevant fractions were concentrated and desalted on a Sephadex G-10 column (600 \times 50 mm) using distilled water as eluent (RI detection). The purity of the oligosaccharides was checked by analytical HPAEC.

Semi-preparative HPAEC was performed using a Dionex LC system with pulsed amperometric detection (PAD), equipped with a CarboPac PA-1 column (250 mm \times 9 mm), eluted with a gradient of NaOAc in 0.1 M NaOH at a flow rate of 4 mL/min. PAD-detection was carried out with a gold working electrode and triple-pulse amperometry was used. Immediately after collection, fractions were neutralized manually with aq 99% HOAc, followed by desalting on a Dowex AG 50W-X12 (100–200 mesh, H⁺-form, Bio-Rad) column (RI detection) using distilled water as eluent, and subsequent lyophilization.

Gas-liquid chromatography.—GLC analyses were performed on a Chrompack CP9002 gas chromatograph, equipped with a CP-Sil 5 CB DFc.25 (Chrompack) capillary column (25 m \times 0.32 mm) using a temperature program of 130–230 °C at 4 °C/min.

Monosaccharide analysis.—Oligosaccharides were subjected to methanolysis (methanolic 1 M HCl, 18 h, 85 °C), and the resulting mix-

tures of methyl glycosides were trimethylsilylated with 1:1:5 hexamethyldisilazane–trimethylchlorosilane–pyridine, and quantitatively analyzed by GLC [17].

Methylation analysis.—Samples were dissolved in 0.5 M NH_4OH (250 μL) containing NaBD_4 (10 mg/mL). After 1 h, the mixture was neutralized with aq 99% HOAc, then concentrated. Boric acid was removed by repetitive co-evaporation with 9:1 MeOH–HOAc and MeOH. Permethylation was carried out essentially as described [18]. Briefly, freshly ground NaOH pellets (250 mg) were added to solutions of samples in Me_2SO (200 μL), and portions of MeI (250 μL) were added after 5, 15, and 25 min. The reaction was stopped after 20 min by adding aq $\text{Na}_2\text{S}_2\text{O}_3$ (1 mL, 100 mg/mL) and CHCl_3 (1 mL). The chloroform layer was extracted with water (3×0.5 mL), then concentrated. After hydrolysis with 2 M CF_3COOH (0.3 mL; 120 °C, 1 h), reduction (see above), acetylation with Ac_2O (0.5 mL; 120 °C, 3 h), quenching with water (0.5 mL), and neutralization with NaHCO_3 , the partially methylated alditol acetates were extracted with CH_2Cl_2 (3×0.7 mL). After concentration to about 20 μL (N_2), samples were analyzed by GLC and GLC–EIMS.

Gas–liquid chromatography–electron impact mass spectrometry (GLC–EIMS).—GLC–EIMS analyses were carried out on a Fisons MD800/8060 system (electron energy, 70 eV; carrier gas, He) equipped with a DB-1 fused-silica capillary column (30 m \times 0.32 mm, J&W Scientific) using a temperature program of 110–240 °C at 4 °C/min followed by isothermal elution for 3 min.

Mass spectrometry.—Approximately 10–25% of the total amount of each fraction was used for mass spectrometric analysis. NaBD_4 -treated and permethylated carbohydrates were dissolved in 1:1 MeOH–aq 1% HCOOH (100 μL) for ESMS. Positive-ion mode ES mass spectra were obtained using a VG Platform II single quadrupole mass spectrometer. Aliquots of 10 μL of the samples were infused into a mobile phase of 1:1 MeOH–aq 1% HCOOH and introduced into the electrospray source at a flow rate of 5 $\mu\text{L}/\text{min}$. Spectra were scanned

at a speed of 8 s for m/z 200–2000, with a cone voltage of 95 V, recorded and processed using the MassLynx software, version 2.0. Mass calibration was performed by multiple-ion monitoring of peracetylated malto-oligosaccharides.

FABMS was carried out using a Jeol JMS-SX/SX102A tandem mass spectrometer (BEBO geometry) at 10 kV accelerating voltage. A Xe beam of about 6 kV translational energy (gun current 10 mA) was used for FAB ionization. The CID tandem mass spectra were obtained by using the collision cell in the third field free region of the mass spectrometer with air as collision gas at a pressure sufficient to reduce the intensity of the selected ion beam by 50%. As the collision cell was held at ground potential, the collision energy in the MS-MS experiments was 10 keV. Spectra were scanned at a speed of 30 s for the full mass range specified by the accelerating voltage used, recorded and averaged using a Hewlett–Packard HP9000 data system running Jeol complement software. NaBD_4 -treated and permethylated carbohydrates were dissolved in 10 μL MeOH and about 1 μL of the solution was mixed with 0.8 μL thioglycerol matrix on the probe tip.

NMR spectroscopy.—Prior to NMR analysis samples were exchanged twice in D_2O (99.9 atom% D, Cambridge Isotope Laboratories, MA, USA) and then dissolved in D_2O (99.96 atom% D, Isotec, USA). NMR spectra were recorded on Bruker AC-300 (Department of Organic Chemistry, Utrecht University), Bruker AMX-500 (Bijvoet Center, Utrecht University), Bruker AMX-600 (Bijvoet Center, Utrecht University or NSR Center, University of Nijmegen) or Varian UNITY-plus 750 (Bijvoet Center, Utrecht University) instruments at probe temperatures of 27 or 5 °C. Chemical shifts for ^1H are expressed in ppm relative to internal acetone (δ 2.225) or acetate (δ 1.908), and for ^{13}C to external glucose (δ Glcp C-1 α 92.9, Glcp C-1 β 96.7 [12]).

1D ^1H NMR spectra were recorded with a sweep width of 5000 Hz at 500 MHz or 6000 Hz at 600 MHz in data sets of 16,384 points. Suppression of the HOD signal was achieved by applying the WEFT pulse as described [19]. Proton decoupled ^{13}C NMR spectra were ac-

quired at 75.469 MHz. Typically, 50,000 transients of 16,384 data points were recorded. All 2D NMR spectra employed the time-proportional phase increment (TPPI) method [20]. Only seHSQC used the STATES-TPPI method [21]. In the 2D homonuclear proton NMR spectra the HOD signal was suppressed using presaturation during a relaxation delay for 1 s. 2D TOCSY spectra were acquired using MLEV 17 mixing sequences of 20–100 ms preceded by a trim pulse of 2.5 ms. The spin-lock field strength corresponded with a 90° pulse of 25–30 μ s and the spectral width was between 4 and 6 ppm in each dimension. Typically, 400–512 experiments of 2048 points were acquired with 4–32 scans per increment. 2D DQF-COSY spectra were recorded with a spectral width as in the 2D TOCSY spectra. Typically, 400–512 free induction decays, each acquired as 8 or 16 transients of 2048 data points were recorded. 2D ROESY spectra were obtained with a mixing time of 200–250 ms. The spin-lock field strength was in accordance with a 90° pulse of 100–120 μ s. The spectral width corresponded with 5–7 ppm in each dimension. Typically, 400–512 experiments of 2048 points were acquired with 32–64 scans per increment. The frequency offset was initially placed on the HOD resonance and switched to about 5.7 ppm just before application of the spin-lock pulse thereby reducing the Hartmann–Hahn transfer during the ROE mixing time [22]. 2D sensitivity enhanced HSQC spectra were proton detected and two gradients were applied for ^{13}C coherence selection. These spectra were acquired with the proton offset at about 4.6 ppm and a sweepwidth of about 6 ppm. In the ^{13}C dimension the offset was placed around 80 ppm and a sweep width of 60 ppm was used. Typically, 300–350 free induction decays of 1024 data points were acquired using 128–256 scans per decay. 2D HMBC spectra were recorded essentially as the 2D seHSQC spectra. The delay for the evolution of the long range couplings was 40–50 ms. NMR data sets were processed using Bruker UXNMR software or the Triton NMR software package (Bijvoet Center, Utrecht University). Briefly, time domain data were multiplied by phase-shifted (squared-)sine-bell

functions or with a Lorentzian-to-Gaussian multiplication. After zerofilling and Fourier transformation datasets of 1024×1024 or 2048×1024 points were obtained, which were baseline corrected with a fourth-order polynomial function when necessary. Accurate chemical shift values obtained from 1D spectra are represented with three (protons) or two (carbons) decimals, whereas values obtained from 2D spectra are depicted with two (protons) or one (carbon) decimals.

Acknowledgements

The authors thank Dr. R.W. Wechselberger (Bijvoet Center, Department of NMR Spectroscopy, Utrecht University, The Netherlands) for recording the 1D ^1H NMR spectra using the Varian Unity plus 750 instrument. This research was supported by the Dutch Technology Foundation (NWO/STW), Gist-brocades, The Product Board for Feeding Stuffs (VVR), and Borculo Whey Products.

References

- [1] N. Onishi, A. Yamashiro, K. Yokozeki, *Appl. Environ. Microbiol.*, 61 (1995) 4022–4025.
- [2] M.A. Levrat, C. Rémésy, C. Demigne, *J. Nutr.*, 121 (1991) 1730–1737.
- [3] T. Yoshida, T. Oowada, A. Ozaki, T. Mizutani, *Biosci. Biotech. Biochem.*, 57 (1993) 1775–1776.
- [4] S. Yanahira, M. Morita, S. Aoe, T. Suguri, Y. Takada, S. Miura, I. Nakajima, *J. Nutr. Sci. Vitaminol.*, 43 (1997) 123–132.
- [5] S. Zarate, M.H. López-Leiva, *J. Food Prot.*, 33 (1990) 262–268.
- [6] N.G. Asp, A. Burvall, A. Dahlqvist, P. Hallgren, A. Lundblad, *Food Chem.*, 5 (1980) 147–153.
- [7] T. Toba, A. Yokota, S. Adachi, *Food Chem.*, 16 (1985) 147–162.
- [8] S. Yanahira, T. Kobayashi, T. Suguri, M. Nakakoshi, S. Miura, H. Ishikawa, I. Nakajima, *Biosci. Biotech. Biochem.*, 59 (1995) 1021–1026.
- [9] T. Usui, S. Morimoto, Y. Hayakawa, M. Kawaguchi, T. Murata, Y. Matahira, Y. Nishida, *Carbohydr. Res.*, 285 (1996) 29–39.
- [10] B. Domon, C.E. Costello, *Glyconconj. J.*, 5 (1988) 397–409.
- [11] V. Kováčik, J. Hirsch, P. Kovác, W. Heerma, J.E. Thomas-Oates, J. Haverkamp, *J. Mass Spectrom.*, 30 (1995) 949–958.
- [12] K. Bock, H. Thøgersen, *Annu. Rep. NMR Spectrosc.*, 13 (1982) 1–57.

- [13] J.F. Espinosa, E. Montero, A. Vian, J.L. García, H. Dietrich, R.R. Schmidt, M. Martín-Lomas, A. Imberty, F.J. Cañada, J. Jiménez-Barbero, *J. Am. Chem. Soc.*, 120 (1998) 1309–1318.
- [14] J.W. van de Vis, M.J.F. Searle-van Leeuwen, H.A. Silha, F.J.M. Kormelink, A.G.J. Voragen, *Carbohydr. Polym.*, 16 (1991) 167–187.
- [15] B.A. Spronk, G.J. Rademaker, J. Haverkamp, J.E. Thomas-Oates, J.-P. Vincken, A.G.J. Voragen, J.P. Kamerling, J.F.G. Vliegthart, *Carbohydr. Res.*, 305 (1997) 233–242.
- [16] M.T. Tollier, J.P. Robin, *Ann. Technol. Agric.*, 28 (1979) 1–15.
- [17] J.P. Kamerling, J.F.G. Vliegthart, in A.M. Lawson (Ed.), *Clinical Biochemistry—Principles, Methods, Applications*, Vol. 1, *Mass Spectrometry*, Walter de Gruyter, Berlin, 1989, pp. 176–263.
- [18] I. Ciucanu, F. Kerek, *Carbohydr. Res.*, 131 (1984) 209–217.
- [19] K. Hård, G. van Zadelhoff, P. Moonen, J.P. Kamerling, J.F.G. Vliegthart, *Eur. J. Biochem.*, 209 (1992) 895–915.
- [20] D. Marion, K. Wüthrich, *Biochem. Biophys. Res. Commun.*, 113 (1983) 967–974.
- [21] D. Marion, M. Ikura, R. Tschudin, A. Bax, *J. Magn. Reson.*, 85 (1989) 393–399.
- [22] B.R. Leeftang, L.M.J. Kroon-Batenburg, *J. Biomol. NMR*, 2 (1992) 495–518.